

## Articles

## Identification of a Novel 4-Aminomethylpiperidine Class of M<sub>3</sub> Muscarinic Receptor Antagonists and Structural Insight into Their M<sub>3</sub> Selectivity

Yufu Sagara,\* Takeshi Sagara, Minaho Uchiyama, Sachie Otsuki, Toshifumi Kimura, Toru Fujikawa, Kazuhito Noguchi, and Norikazu Ohtake

Tsukuba Research Institute, Banyu Pharmaceutical Co., Ltd., 3 Okubo, Tsukuba, Ibaraki 300-2611, Japan

Received November 30, 2005

Identification of a novel class of potent and highly selective M<sub>3</sub> muscarinic antagonists is described. First, the structure–activity relationship in the cationic amine core of our previously reported triphenylpropionamide class of M<sub>3</sub> selective antagonists was explored by a small diamine library constructed in solid phase. This led to the identification of M<sub>3</sub> antagonists with a novel piperidine pharmacophore and significantly improved subtype selectivity from a previously reported class. Successive modification on the terminal triphenylpropionamide part of the newly identified class gave **14a** as a potent M<sub>3</sub> selective antagonist that had >100-fold selectivity versus the M<sub>1</sub>, M<sub>2</sub>, M<sub>4</sub>, and M<sub>5</sub> receptors (M<sub>3</sub>: K<sub>i</sub> = 0.30 nM, M<sub>1</sub>/M<sub>3</sub> = 570-fold, M<sub>2</sub>/M<sub>3</sub> = 1600-fold, M<sub>4</sub>/M<sub>3</sub> = 140-fold, M<sub>5</sub>/M<sub>3</sub> = 12000-fold). The possible rationale for its extraordinarily higher subtype selectivity than reported M<sub>3</sub> antagonists was hypothesized by sequence alignment of multiple muscarinic receptors and a computational docking of **14a** into transmembrane domains of M<sub>3</sub> receptors.

### Introduction

Acetylcholine (ACh) exerts a variety of pharmacological activities via nicotinic and muscarinic receptors distributed peripherally and centrally. There are five muscarinic receptor subtypes (M<sub>1</sub>–M<sub>5</sub>) identified so far.<sup>1</sup> Although these receptor subtypes have been proposed to participate in a number of physiologic actions,<sup>2</sup> the precise roles of each receptor subtype in the specific muscarinic actions of ACh remain to be elucidated. Recent developments of transgenic mice lacking each of the M<sub>1</sub>–M<sub>5</sub> receptors help to clarify some of their functions;<sup>3</sup> however, pharmacological studies using truly subtype-selective ligands are also important. Furthermore, muscarinic receptors seem to be involved in many diseases and nonselective muscarinic receptor ligands have been used as therapeutic agents. However, these therapeutic agents often cause undesirable side effects partly due to their nonselective profiles or the wide distribution of the muscarinic receptors.<sup>4</sup>

Since M<sub>1</sub>–M<sub>5</sub> receptors are homologous across receptor subtypes as well as across mammalian species,<sup>5</sup> identification of truly selective antagonists or agonists can still be challenging. Efforts are continued to identify selective muscarinic ligands in pharmaceutical research because of needs for both pharmacological tools to clarify the roles of each receptor subtype and better therapeutic agents.<sup>6</sup>

We previously discovered a novel triphenylpropionamide class of M<sub>3</sub> antagonists with good M<sub>3</sub> binding affinity and remarkable subtype selectivity by a combinatorial library approach.<sup>7</sup> Among them, the antagonist possessing a unique L-Pro-D-Pro spacer, represented by **1**, was subjected to further chemical modification and L-(R)-hydroxyproline(Hyp)-D-Pro analogues **2a** and **2b** were identified as M<sub>3</sub> antagonists with improved subtype selectivity (Table 1).<sup>8</sup>

In this paper, we will describe the results of structural alteration in the diamine core structure of the novel M<sub>3</sub>

**Table 1.** Triphenylpropionamide Class of M<sub>3</sub> Antagonists

compd	binding affinity (K <sub>i</sub> , nM) <sup>a</sup> (subtype selectivity over M <sub>3</sub> receptors)				
	M <sub>3</sub>	M <sub>1</sub>	M <sub>2</sub>	M <sub>4</sub>	M <sub>5</sub>
<b>1</b>	99 <sup>b</sup> (1.0)	>2500 <sup>c</sup> (>25)	3100 <sup>b</sup> (31)	>1700 <sup>c</sup> (>17)	>5000 <sup>c</sup> (>51)
<b>2a</b>	23 <sup>b</sup> (1.0)	>2500 <sup>c</sup> (>110)	6400 <sup>b</sup> (280)	740 <sup>b</sup> (32)	>5000 <sup>c</sup> (>220)
<b>2b</b>	1.5 ± 0.1 (1.0)	1300 ± 0 (870)	270 ± 15 (180)	57 ± 2 (38)	3500 ± 310 (2300)
atropine	0.50 ± 0.01 (1.0)	0.25 ± 0.02 (0.50)	1.5 ± 0.1 (3.0)	0.34 ± 0.02 (0.68)	0.54 ± 0.03 (1.1)

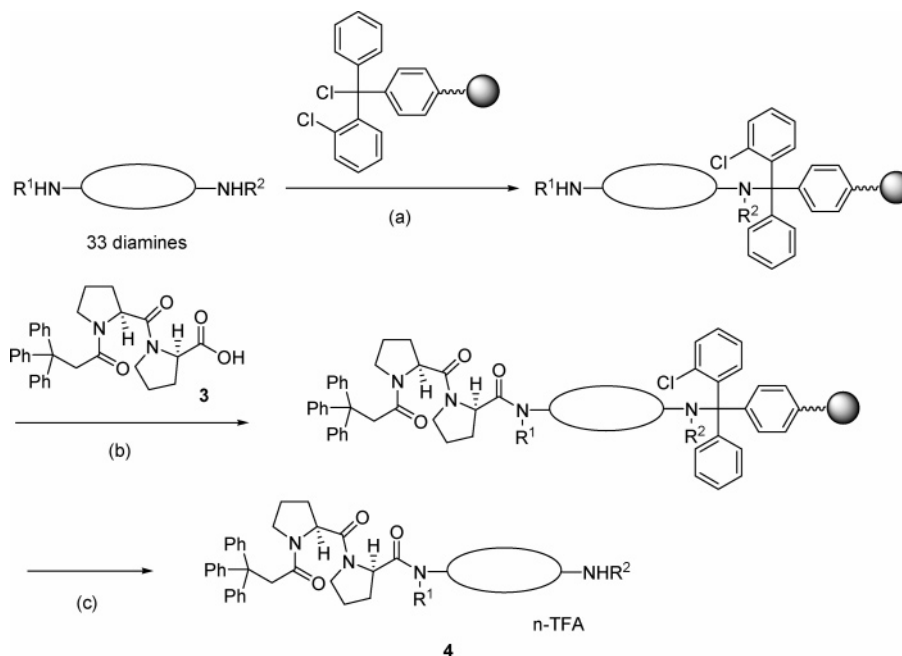
<sup>a</sup> K<sub>i</sub> values are expressed as the mean ± standard error of the mean (SEM), for the compounds which were tested three or more times. <sup>b</sup> When only two separate experiments were performed, values are expressed as the mean of duplicate determinations, and the variances between determinations were less than ±11%. <sup>c</sup> Values are expressed as the mean of duplicate determinations.

antagonists with L-Pro-D-Pro spacer and the identification of **14a** with a new 4-aminomethylpiperidine core structure that had sub-nanomolar M<sub>3</sub> affinity and >100-fold selectivity versus the M<sub>1</sub>, M<sub>2</sub>, M<sub>4</sub>, and M<sub>5</sub> receptors. In addition, an attempt to understand the structural basis of the selective recognition of M<sub>3</sub> receptors by **14a** was also made using a computational modeling technique.

### Chemistry

Structural alteration in the diamine core part of **1** was explored by constructing a small library of analogues with diverse diamine structures.

\* To whom correspondence should be addressed. Tel.: +81-29-877-2000. Fax: +81-29-877-2029. E-mail: yufu\_sagara@merck.com.

**Scheme 1.** Construction of Diamine Library Using Solid Phase Parallel Synthesis<sup>a</sup>

<sup>a</sup> Reagents and conditions: (a) see Supporting Information; (b) PyBOP, DIEA, DMF; (c) 50% DCM-TFA.

To maximize the efficiency in exploring structural diversity in the diamine core part, we designed high-throughput chemistry as shown in Scheme 1.

The library synthesis was started by solid phase immobilization of diverse diamine reagents, as it allows us to operate selective protection and deprotection of diamine functionalities. 2-Chlorotrityl chloride resin (Cl-Trt(2-Cl)-resin)<sup>9</sup> was found to proceed immobilization of the selected diamine set effectively.<sup>10</sup>

The solution phase synthesis of monoprotected diamines by protective groups such as Boc, Cbz, or benzyl group usually requires lengthy and laborious steps involving conversion of other functional groups into amine groups. However, solid phase immobilization of diamines makes it easier to selectively protect one of the diamine functionalities to leave the other group as the site for amide condensation with (2*R*)-1-[(2*S*)-1-(3,3,3-triphenylpropanoyl)pyrrolidine-2-yl]carbonylpyrrolidine-2-carboxylic acid (**3**) in Scheme 1. The amide condensation reaction proceeded cleanly in the PyBOP/diisopropylethylamine (DIEA)/DMF system.<sup>11</sup> Finally, the target molecules **4** were cleaved off from the resin by acid treatment. After cleavage from the resin, most of the samples except a few showed more than 90% purity by LC-MS and HPLC spec.<sup>12</sup>

Subsequently, replacement of the L-Pro-D-Pro spacer in the novel diamine analogues by L-Hyp-D-Pro spacer and further modification in the terminal triphenylpropionamide part and *N*-substituents of the diamine core part were performed to give the analogues with the optimal selectivity profiles. All the reactions for the analogue synthesis were performed by conventional solution phase chemistry.

As an example, preparation of **14a** and its *N*-alkylated tertiary amine derivatives **15a–15g** is shown in Scheme 2.<sup>13</sup> Methyl esterification of commercially available *D*-benzyloxycarbonylproline **5** followed by deprotection of benzyloxy group (*Z*) and subsequent amidation with *N*- $\alpha$ -benzyloxycarbonyl-*O*-*tert*-butyl-L-4-*trans*-hydroxyproline (*Z*-Hyp(*t*Bu)-OH) gave **8**. This monoamide **8** was transformed to diamide **11** by deprotection and condensation with tris(4-fluorophenyl)propionic acid (**10**). Hydrolysis of **11** and subsequent coupling with 4-aminomethyl-1-*tert*-butoxycarbonylpiperidine<sup>14</sup> afforded triamide **13**. Depro-

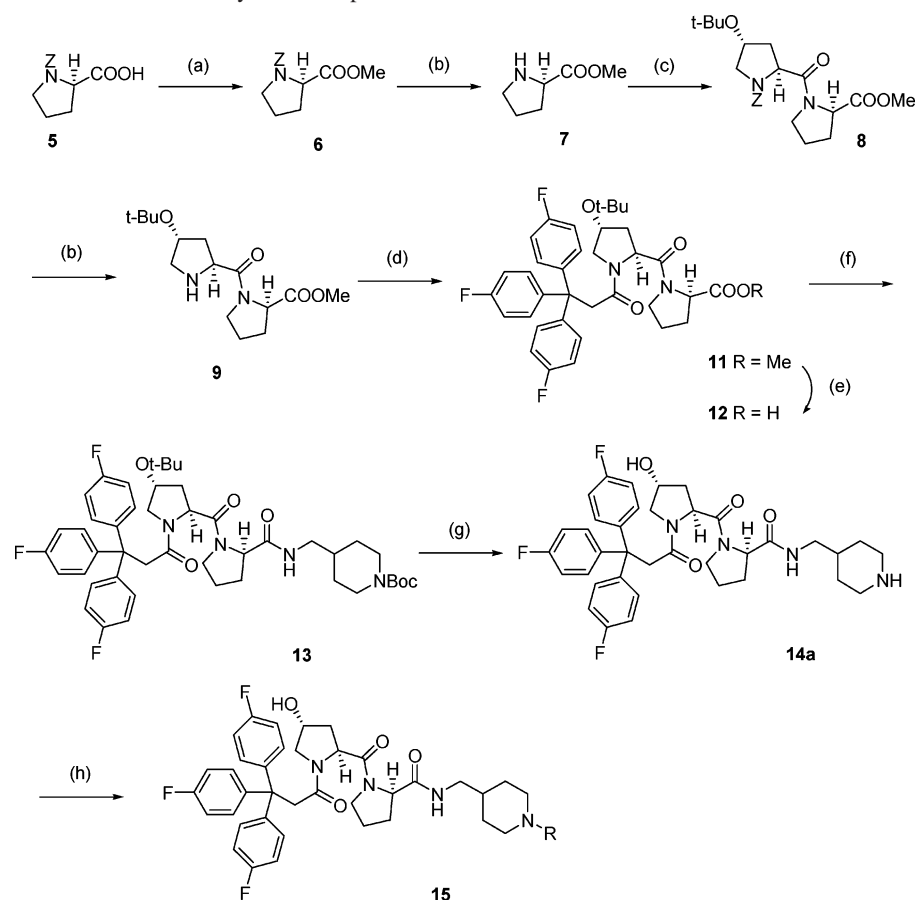
tection of both *tert*-butoxycarbonyl and *tert*-butyl groups of **13** by treatment with TFA afforded **14a**. Finally, either reductive amination<sup>15</sup> or alkylation of **14a** with appropriate alkylating reagents provided the *N*-alkylated compounds **15a–15g**. Analogues **14b** and **14c** were prepared by similar procedure using the appropriate *tert*-butoxycarbonyl-protected diamine instead of 4-aminomethyl-1-*tert*-butoxycarbonylpiperidine. Chlorine-substituted triphenylpropionamide compounds (**52a–52c**) and nonsubstituted triphenylpropionamide compounds (**2a**, **51a–51c**) were also prepared similarly using commercially available tris(4-chlorophenyl)propionic acid or triphenylpropionic acid, respectively, instead of **10**, in combination with appropriate *tert*-butoxycarbonyl-protected diamines.

Tris(4-fluorophenyl)propionic acid (**10**) used in the preparation of **14a–14c** and **15a–15g** was synthesized as shown in Scheme 3. Condensation reaction of tris(4-fluorophenyl)carbinol (**16**) with cyanoacetic acid proceeded cleanly to give tris(4-fluorophenyl)propionitrile (**17**) according to the procedures slightly modified from the original methods reported in the synthesis of tris(4-chlorophenyl) propionitrile.<sup>16</sup> Hydrolysis of **17** gave the target compound **10** in quantitative yield with high purity.<sup>17</sup>

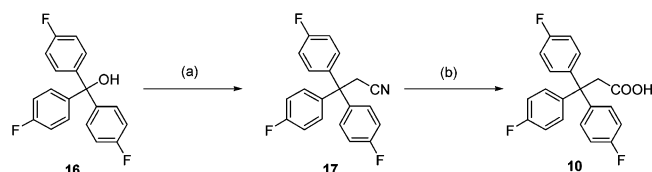
## Results and Discussion

We chose 33 diamine building blocks from commercially available reagents and the diamines easily prepared from commercially available precursors to display maximum structural diversity (Table 2). The 33 crude products prepared in the solid phase amide condensation reaction were assayed at 1  $\mu$ M to measure their inhibition (%) of M<sub>3</sub> binding of *N*-methylscopolamine (NMS). As shown in Table 2, the piperidine derivatives (**29**, **30**, **32**, and **37**) and cyclohexyldiamine derivatives (**39** and **41**) displayed high inhibitory activities (>50%), and their *K*<sub>i</sub> values were determined by independent titration assays. Among them, the compounds **30**, **32**, **37**, and **41** showed a higher *K*<sub>i</sub> value than that of the reference compound **1**.

M<sub>3</sub> binding affinities of the newly identified diamine core part in **30**, **32**, **37**, and **41** were further examined by testing their L-Hyp-D-Pro spacer analogues. Because of the difficulty

**Scheme 2.** Preparation of **14a** and Its *N*-Alkylated Compounds **15**<sup>a</sup>

<sup>a</sup> Reagents and conditions: (a) DMAP, MeOH, WSC, CHCl<sub>3</sub> (78%); (b) H<sub>2</sub>, Pd(OH)<sub>2</sub>, MeOH; (c) Z-Hyp(*t*Bu)-OH, WSC, HOBT, CHCl<sub>3</sub> (50%, two steps); (d) **10**, WSC, HOBT, DIEA, CHCl<sub>3</sub> (86%, two steps); (e) NaOH (aq), MeOH; (f) 4-aminomethyl-1-*t*-butoxycarbonylpiperidine, WSC, HOBT, CHCl<sub>3</sub> (85%, two steps); (g) TFA (neat) (quant.); (h) aldehyde, NaBH<sub>3</sub>CN–ZnCl<sub>2</sub>, MeOH, rt; or RX, K<sub>2</sub>CO<sub>3</sub>, CH<sub>3</sub>CN, heat.

**Scheme 3.** Preparation of Tris(4-fluorophenyl)propionic Acid **10**<sup>a</sup>

<sup>a</sup> Reagents and conditions: (a) cyanoacetic acid, zinc chloride, AcOH at 130 °C, 6.5 h (61%); (b) conc HCl, conc H<sub>2</sub>SO<sub>4</sub>, AcOH at 130 °C, 44 h (quant.).

in separation of the diastereomers of the 1,2-cyclohexanediamine derivative, we only succeeded in preparation of **51a**, **51b**, and **51c** and tested their M<sub>3</sub> binding affinities and subtype selectivities (Table 3). These derivatives showed higher M<sub>3</sub> binding affinities and selectivity than the reference compound **2a** with 3(*S*)-aminomethyl piperidine structure. Especially, **51a** with a 4-aminomethylpiperidine diamine core part was found to demonstrate >100-fold selectivity versus M<sub>1</sub>, M<sub>2</sub>, M<sub>4</sub>, and M<sub>5</sub> receptors.

Optimization of the triphenylpropionamide part of the newly identified diamine analogues was next carried out (Table 3). In comparison with **51a**–**51c**, introduction of chlorine atom onto each of the phenyl rings generally increased M<sub>3</sub> binding affinity in all diamine derivatives (**52a**–**52c**), and especially **52a** exhibited stronger M<sub>3</sub> binding affinity than **51a** by 10-fold. However, **52b** and **52c** had slightly lower subtype selectivity. In the case of fluorine-substituted triphenylpropionamide analogues, all three compounds **14a**, **14b**, and **14c** showed

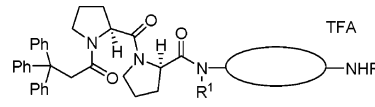
improvements in M<sub>3</sub> binding affinity by 10-fold, when compared to nonsubstituted analogues **51a**–**51c**. More interestingly, subtype-selectivity profiles of **14a**, **14b**, and **14c** were greatly improved, and **14a** could be the most selective M<sub>3</sub> antagonist among the ones reported so far.<sup>18</sup>

The effect of piperidine *N*-substituents of **14a** on M<sub>3</sub> binding affinity and subtype selectivity was also examined (Table 4). To avoid significant increase of the molecular weight and hydrophobicity of the molecules, relatively small substituents were examined.

All the tested *N*-substituted derivatives retained good M<sub>3</sub> binding affinity and selectivity. The cyclopropylmethyl (**15c**) and cyclopentylmethyl (**15e**) derivatives exhibited higher M<sub>3</sub> binding affinity than **14a**, but they showed no improvements in their selectivity profiles.

As the result of chemical modification in the diamine core part, the terminal triphenylpropionamide part, and the piperidine *N*-substituents, five compounds—**14a**, **14c**, **15b**, **15c**, and **52a**—were identified to show sub-nanomolar M<sub>3</sub> binding affinity and >100-fold selectivity versus the M<sub>1</sub>, M<sub>2</sub>, M<sub>4</sub>, and M<sub>5</sub> receptors.

Among them, **14a** with the highest M<sub>3</sub> selectivity was subjected to further evaluation using an *in vitro* system with rat tissues<sup>19</sup> to obtain the information on the mechanism of action. In the isolated rat trachea, **14a** (0.3–3 nM) effectively antagonized the carbachol-induced responses in a dose-dependent manner (Figure 1). Schild analysis yielded a slope of 1.08 ± 0.16, suggesting a competitive antagonism for this compound and a pA<sub>2</sub> value of 9.65 ± 0.10 in good agreement with the binding value<sup>20</sup> (Figure 1, inset). Compound **14a** also exhibited

**Table 2.** Results of One-Point Screening of Diamine Library (Percent Inhibition of M<sub>3</sub> Binding of NMS) and K<sub>i</sub> Values of the Selected Compounds<sup>a</sup>


No.	diamine structure	inhibition at 1 $\mu$ M	M <sub>3</sub> K <sub>i</sub>	No.	diamine structure	inhibition at 1 $\mu$ M	M <sub>3</sub> K <sub>i</sub>	No.	diamine structure	inhibition at 1 $\mu$ M	M <sub>3</sub> K <sub>i</sub>
18		-4%		30		82%	49 nM	42		11%	
19		2%		31		32%		43		0	
20		12%		32		91%	23 nM	44		8%	
21		-2%		33		33%		45		5%	
22		7%		34		7%		46		10%	
23		7%		35		5%		47		12%	
24		4%		36		28%		48		6%	
25		22%		37		88%	29 nM	49		9%	
26		12%		38		-7%		50		6%	
27		-4%		39		59%	170 nM				
28		0		40		40%					
29		59%	150 nM	41		80%	48 nM	1		74%	99 nM

<sup>a</sup>Single determination for all values (inhibition percent and M<sub>3</sub> K<sub>i</sub>).

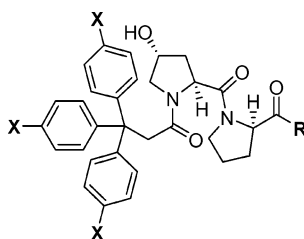
no intrinsic activity at the receptor by compound alone. In the isolated rat atria, **14a** showed less potent inhibition of carbachol-induced bradycardia, with a pA<sub>2</sub> value of 6.69 ± 0.13 and a slope of 1.04 ± 0.12 (Figure 2). These results indicated that **14a** was a competitive antagonist at M<sub>2</sub> and M<sub>3</sub> receptors, and the functional selectivity of this compound was 910-fold greater for tracheal M<sub>3</sub> receptors over cardiac M<sub>2</sub> receptors in rat, which was in good agreement with the selectivity observed in the binding assay.

**Modeling of Selective Recognition in M<sub>3</sub> Receptors.** To understand the structural basis of the observed selectivity of our M<sub>3</sub> antagonists, the selective binding mode of this new class in M<sub>3</sub> receptors was hypothesized. To this end, we first analyzed amino acid sequence difference among muscarinic receptor subtypes (Figure 3). Although extremely high sequence identity in transmembrane (TM) regions was observed among muscarinic subtypes (73–83% identity), three unique amino acid residues, Asn138, Lys523, and Asn527 in M<sub>3</sub> receptor, were identified in the upper region of TM3 and TM7. As these three residues are completely nonconserved among the predicted TM domains of muscarinic receptor subtypes, it might be possible

to assume that the novel antagonist class may specifically recognize these residues to achieve the observed good subtype selectivity.

To validate the hypothesis computationally, modeling of the M<sub>3</sub> receptor and its docking with a novel antagonist **14a** was attempted. The TM domains of the M<sub>3</sub> receptor were modeled using an X-ray crystal structure of bovine rhodopsin as a template. In the M<sub>3</sub> receptor model, the three amino acid residues identified by multiple sequence alignment were found on the inner surface of TM3 and TM7 to create a potential binding pocket for small ligand molecules. Therefore, we hypothesized that these three residues might have M<sub>3</sub> specific interactions with antagonist molecules bound in the cleft surrounded by seven TM helices.

To obtain further insights for the hypothesis, a highly selective M<sub>3</sub> antagonist **14a** was docked into the receptor model. The docking experiment was carried out by the following steps. (1) Assuming that the cationic N center of **14a** interacts with the carboxylate group of Asp148 in TM3 through an ionic bond,<sup>21,22</sup> a variety of conformations of **14a** were generated and manually docked into the receptor model. (2) The conformations of **14a**

**Table 3.** Binding Profiles of the Compounds with the Newly Identified Diamine Core Parts and Various Substituents on the Triphenylpropionamide Part

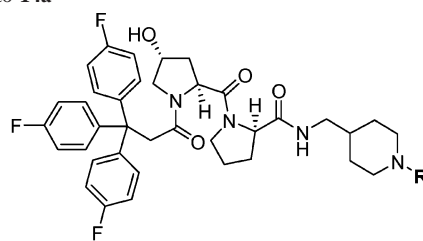
No.	X	R	Binding Affinity ( $K_i$ , nM) <sup>a</sup> (Subtype Selectivity over M <sub>3</sub> receptors)				
			M <sub>3</sub>	M <sub>1</sub>	M <sub>2</sub>	M <sub>4</sub>	M <sub>5</sub>
51a	H		4.2 <sup>b</sup> (1.0)	1800 <sup>b</sup> (430)	3000 <sup>b</sup> (710)	480 <sup>b</sup> (110)	> 5100 <sup>c</sup> (> 1200)
51b	H		2.8 <sup>b</sup> (1.0)	2000 <sup>b</sup> (710)	1200 <sup>b</sup> (430)	150 <sup>b</sup> (54)	> 5100 <sup>c</sup> (> 1800)
51c	H		3.7 <sup>b</sup> (1.0)	> 2600 <sup>c</sup> (> 700)	3700 <sup>b</sup> (1000)	290 <sup>b</sup> (78)	> 5100 <sup>c</sup> (> 1400)
52a	Cl		0.39 <sup>b</sup> (1.0)	93 <sup>b</sup> (240)	310 <sup>b</sup> (790)	53 <sup>b</sup> (140)	2500 <sup>b</sup> (6400)
52b	Cl		1.2 <sup>b</sup> (1.0)	260 <sup>b</sup> (220)	94 <sup>b</sup> (78)	24 <sup>b</sup> (20)	950 <sup>b</sup> (790)
52c	Cl		1.6 <sup>b</sup> (1.0)	460 <sup>b</sup> (290)	100 <sup>b</sup> (630)	120 <sup>b</sup> (75)	2700 <sup>b</sup> (1700)
14a	F		0.30 ± 0 (1.0)	170 ± 18 (570)	490 ± 33 (1600)	42 ± 4 (140)	3500 ± 310 (12000)
14b	F		0.48 <sup>b</sup> (1.0)	300 <sup>b</sup> (630)	220 <sup>b</sup> (460)	29 <sup>b</sup> (60)	1700 <sup>b</sup> (3500)
14c	F		0.39 ± 0.04 (1.0)	300 ± 23 (770)	450 ± 27 (1200)	39 ± 4 (100)	1700 ± 120 (4400)

<sup>a</sup>  $K_i$  values are expressed as the mean ± standard error of the mean (SEM), for the compounds which were tested three or more times. <sup>b</sup> When only two separate experiments were performed, values are expressed as the mean of duplicate determinations, and the variances between determinations were less than ±21%. <sup>c</sup> Values are expressed as the mean of duplicate determinations.

displaying reasonable interactions with three residues, Asn138, Lys523, and Asn527, were prioritized. (3) The resultant complex structures were then minimized and subjected to visual inspections without further modification. As a result, **14a** gave a limited number of binding conformations in the receptor model to meet the above criteria, and an example of the final complex model is shown in Figure 4. In the complex model, in addition to the salt bridge between the cationic N center of **14a** and the carboxylate group of Asp148, formation of a hydrogen bonding interaction between the hydroxy group of Hyp and the amide group in the side chain of Asn527 and interactions between two 4-fluorophenyl groups in the triphenylpropionamide part of **14a** and the side chains of Asn138 and Lys523

were observed. As discussed previously, introduction of hydroxy group to the amino acid spacer part (substitution of L-Pro with L-Hyp) and fluoro atoms to the triphenylpropionamide part significantly improved the binding affinity and subtype selectivity of the novel antagonist class. All three interactions predicted between **14a** and M<sub>3</sub> receptor in our docking model might explain the observed structure–activity relationship (SAR).

The present docking model is also in good agreement with our hypothesis for subtype selectivity. In the complex model, the terminal triphenylpropionamide part and Hyp-Pro spacer part connecting the diamine core part and the terminal triphenylpropionamide part of **14a** were predicted to make reasonable interactions with all three nonconserved residues among the

**Table 4.** Introduction of Piperidine *N*-Substituents to **14a**<sup>a</sup>

No.	R	Binding Affinity ( $K_i$ , nM) <sup>a</sup> (Subtype Selectivity over $M_3$ receptors)				
		$M_3$	$M_1$	$M_2$	$M_4$	$M_5$
15a	Me	0.51 ± 0.05 (1.0)	270 ± 23 (530)	730 ± 15 (1400)	41 ± 6 (80)	1600 ± 240 (3100)
15b	Et	0.92 <sup>b</sup> (1.0)	580 <sup>b</sup> (630)	1300 <sup>b</sup> (1400)	92 <sup>b</sup> (100)	2800 <sup>b</sup> (3000)
15c		0.17 <sup>b</sup> (1.0)	65 <sup>b</sup> (380)	73 <sup>b</sup> (430)	20 <sup>b</sup> (120)	1600 <sup>b</sup> (9400)
15d		0.53 <sup>b</sup> (1.0)	220 <sup>b</sup> (420)	68 <sup>b</sup> (130)	31 <sup>b</sup> (58)	3100 <sup>b</sup> (5800)
15e		0.19 <sup>b</sup> (1.0)	71 <sup>b</sup> (370)	19 <sup>b</sup> (100)	11 <sup>b</sup> (58)	940 <sup>b</sup> (4900)
15f		2.4 <sup>b</sup> (1.0)	800 <sup>b</sup> (330)	1500 <sup>b</sup> (630)	180 <sup>b</sup> (75)	> 5400 <sup>c</sup> (> 2300)
15g		0.51 <sup>b</sup> (1.0)	210 <sup>b</sup> (410)	110 <sup>b</sup> (220)	48 <sup>b</sup> (94)	3200 <sup>b</sup> (6300)
14a	H	0.30 ± 0 (1.0)	170 ± 18 (570)	490 ± 33 (1600)	42 ± 4 (140)	3500 ± 310 (12000)

<sup>a</sup>  $K_i$  values are expressed as the mean ± standard error of the mean (SEM), for the compounds which were tested three or more times. <sup>b</sup> When only two separate experiments were performed, values are expressed as the mean of duplicate determinations, and the variances between determinations were less than ±18%. <sup>c</sup> Values are expressed as the mean of duplicate determinations.

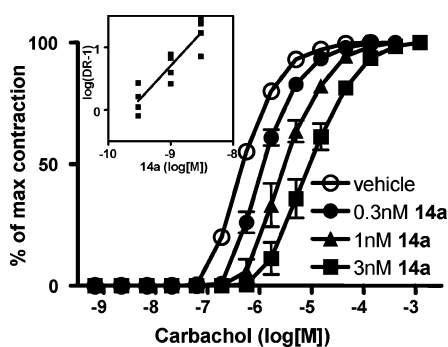


**Figure 1.** Inhibition by **14a** on contractile response induced by carbachol in isolated rat trachea. Data represent the mean ± SEM of four experiments per each dose. The inset shows the Schild regression analysis of the data.

muscarinic receptor subtypes, Asn138, Lys523, and Asn527, simultaneously. As these substructures are not found in the reported  $M_3$  antagonist class, they may interact specifically with these residues to establish highly selective binding to  $M_3$  receptors.

As the complex model is preliminary and not enough to explain the details of the SARs in our novel lead class, further experimental research is required to validate our hypothesis.

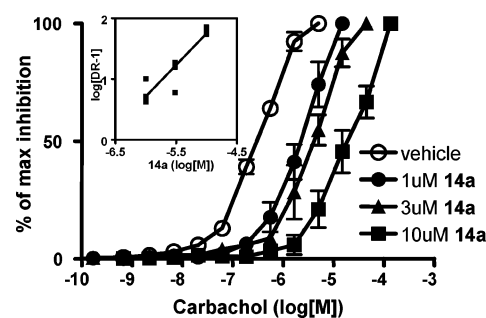


**Figure 2.** Inhibition by **14a** on carbachol-induced bradycardia in isolated rat right atria. Data represent the mean ± SEM of four experiments per each dose. The inset shows the Schild regression analysis of the data.

One of the possible approaches to achieve this is the site-directed mutagenesis experiment. The mutant  $M_3$  receptors altering the aforementioned nonconserved residues may give useful information when their binding profiles with our  $M_3$  selective antagonists are carefully examined. These trials in combination with further chemical modification of this novel  $M_3$  antagonist class may lead to rational identification of selective muscarinic receptor antagonists and agonists.

TM1		
ACM1_HUMAN	(233)	WQVAFIGITGTLGLSLATVGNLLVLSFKV
ACM2_HUMAN	(211)	FEVVVFLVAGLSLVTIIIGNILVWVSLKV
ACM3_HUMAN	(466)	WQVVPIAFLTGILALVLTIIIGNILVWVSPKV
ACM4_HUMAN	(30)	VEVVVPIAFLTGILALVLTIIIGNILVWVSLKV
ACM5_HUMAN	(28)	WEVVTIAAVTAVVSLITIVGNVLMVLSFKV
OPSD_BOVIN	(35)	WQFSLMRLAAYMFLMLLMLGFFINFLTLVTVQ
TM2		
ACM1_HUMAN	(59)	VNNYPLLSLACADLIIGTFGMNLYTTLML
ACM2_HUMAN	(57)	VNNYPLLSLACADLIIGTFGMNLYTTLVI
ACM3_HUMAN	(102)	VNNYPLLSLACADLIIGTFGMNLYTTLIIM
ACM4_HUMAN	(66)	VNNYPLLSLACADLIIGTFGMNLYTTLIIM
ACM5_HUMAN	(64)	VNNYPLLSLACADLIIGTFGMNLYTTLIIM
OPSD_BOVIN	(71)	PLNYTLLNLAVALDFMVFVGGFTTTLTSLN
TM3		
ACM1_HUMAN	(95)	LACDLWLALDYVNASVSMNLLVLSFDRYFVTRP
ACM2_HUMAN	(93)	VVCDLWLALDYVNASVSMNLLVLSFDRYFVTRP
ACM3_HUMAN	(138)	LACDLWLALDYVNASVSMNLLVLSFDRYFVTRP
ACM4_HUMAN	(102)	VVCDLWLALDYVNASVSMNLLVLSFDRYFVTRP
ACM5_HUMAN	(100)	LACDLWLALDYVNASVSMNLLVLSFDRYFVTRP
OPSD_BOVIN	(107)	TGCNLEGGFATLGGELALWLVVLAIBRYVVKCP
TM4		
ACM1_HUMAN	(139)	TPRRAALMIGLAWLVSFVLWAPAI
ACM2_HUMAN	(137)	TTKAGMMAIAAWVLSFVLWAPAI
ACM3_HUMAN	(182)	TTKAGVMIGLAWLVSFVLWAPAI
ACM4_HUMAN	(146)	TTKAGMMAIAAWVLSFVLWAPAI
ACM5_HUMAN	(144)	TPKRAIMIGLAWLVSFVLWAPAI
OPSD_BOVIN	(149)	GENHAIMGVAPTVMWLACAAAPP
TM5		
ACM1_HUMAN	(184)	SQPIITFGTAAAFYLPVTVMCTLYWRI
ACM2_HUMAN	(182)	SNAAVTFGTAAAFYLPVIMTLYWHI
ACM3_HUMAN	(227)	SEPTITFGTAAAFYLPVIMTLYWRI
ACM4_HUMAN	(191)	SNPAVTFGTAAAFYLPVIMTLYWHI
ACM5_HUMAN	(189)	SEPTITFGTAAAFYLPVIMTLYWRI
OPSD_BOVIN	(199)	NNSEPIYMFVVFHFIIPLVIFVFCYQGL
TM6		
ACM1_HUMAN	(361)	EKAARTLSAILLAFILTWTPYNIIMVLVSTFC
ACM2_HUMAN	(383)	EKVTRTILAILLAFIITWAPYNIIMVLVSTFC
ACM3_HUMAN	(487)	EKAARTLSAILLAFIITWTPYNIIMVLVSTFC
ACM4_HUMAN	(396)	EKVTRTILAILLAFIITWTPYNIIMVLVSTFC
ACM5_HUMAN	(438)	EKAARTLSAILLAFIITWTPYNIIMVLVSTFC
OPSD_BOVIN	(246)	AEVTRMVIIMVIAFLICWLPYAGVAFYIFTH
TM7		
ACM1_HUMAN	(397)	TLW RGYWLCYVNSTINPFCYALCNK
ACM2_HUMAN	(419)	TVW TGYWLCYVNSTINPFCYALCNK
ACM3_HUMAN	(523)	TFW RGYWLCYVNSTINPFCYALCNK
ACM4_HUMAN	(432)	TVW RGYWLCYVNSTINPFCYALCNK
ACM5_HUMAN	(474)	TLW RGYWLCYVNSTINPFCYALCNK
OPSD_BOVIN	(285)	IPM TPAFAFKTSAVYVPIVIMMKN

**Figure 3.** Alignment of the sequences of bovine rhodopsin (OPSD\_BOVIN) and the human muscarinic receptors (ACM\_HUMAN).

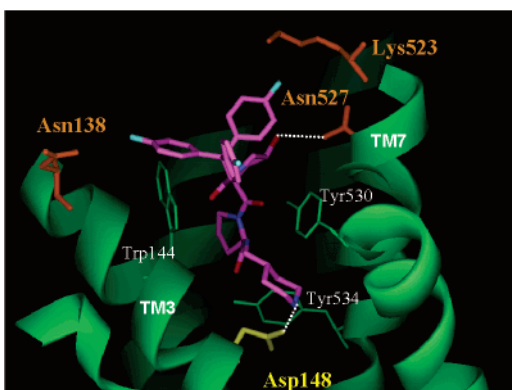


**Figure 4.** Three-dimensional model for binding of **14a** (magenta) in M<sub>3</sub> receptor. Amino acid residues involved in ligand binding are indicated.

## Conclusion

A novel triphenylpropionamide class of M<sub>3</sub> selective antagonists with L-Pro-D-Pro spacer was chemically modified in a stepwise manner. In the first step, we turned our attention to the modification of an important diamine core part. Using solid phase synthesis, we identified the compounds with the novel piperidine pharmacophores showing significantly improved M<sub>3</sub> binding affinity and subtype selectivity.

Introduction of chlorine or fluorine atoms onto the phenyl rings of the terminal triphenylpropionamide part further enhanced M<sub>3</sub> binding affinity and subtype selectivity. Among them, **14a** achieved sub-nanomolar M<sub>3</sub> binding affinity and >100-fold selectivity versus the M<sub>1</sub>, M<sub>2</sub>, M<sub>4</sub>, and M<sub>5</sub> receptors. The functional assay using isolated rat tissue suggested that **14a** was a competitive antagonist, and high M<sub>2</sub>/M<sub>3</sub> functional selectivity was also observed.

The mechanism for the observed selectivity of these novel M<sub>3</sub> antagonists was hypothesized by amino acid sequence

alignment of multiple muscarinic receptor subtypes and computational modeling of selective recognition of M<sub>3</sub> receptor by our antagonist **14a**. Although the model was preliminary and not enough for clear understanding of the mechanism, it was postulated that nonconserved residues among the muscarinic receptor subtypes could be specifically recognized by highly selective M<sub>3</sub> antagonists. Finally, as this class of M<sub>3</sub> antagonists is potent and highly subtype-selective, pharmacological evaluation of this class of compounds to clarify the roles of M<sub>3</sub> receptors and, furthermore, examination of their potential as lead structures for orally available drugs are also in progress. These results will be reported elsewhere.

## Experimental Section

**General Information.** All reagents and solvents were of commercial quality and used without further purification unless otherwise noted. Melting points were determined with a Yanaco MP micromelting point apparatus and were not corrected. <sup>1</sup>H NMR spectra were obtained on a Varian Gemini-300 with tetramethylsilane as an internal standard. Mass spectrometry was performed with a JEOL JMS-SX 102A. TLC was done using Merck Kieselgel F<sub>254</sub> precoated plates. Silica gel column chromatography was carried out on Wako gel C-200. The purity of all target compounds was checked using reversed phase HPLC (C<sub>18</sub> column: YMC-Pack Pro C18, 4.6 × 250 mm, s-5μm) with two diverse solvent systems: system A—compounds were eluted using a linear gradient of 10–90% B/A over 30 min at a flow rate of 1.0 mL/min, where solvent A was aqueous 0.016% H<sub>2</sub>SO<sub>4</sub> and solvent B was CH<sub>3</sub>CN; system B—compounds were eluted using a linear gradient of 20–95% B/A over 30 min at a flow rate of 1.0 mL/min, where solvent A was aqueous 0.016% H<sub>2</sub>SO<sub>4</sub> and solvent B was CH<sub>3</sub>OH.

**General Procedure for the Reaction of Resin Bound Amines with the Carboxylic Acid **3** and Cleavage of Product **4** from Solid Support.** The resin bound amine (ca. 20 mg, ca. 0.020 mmol) was suspended in DMF (300 μL) in a reservoir with a frit, and carboxylic acid **3** (29.8 mg, 0.060 mmol), PyBOP (31.2 mg, 0.060 mmol), and DIEA (20.9 μL, 0.12 mmol) were added. The mixture was left on the orbital shaker for 5 h. DMF (200 μL) was added to the mixture, and the mixture was left on the orbital shaker for additional 18 h. Reaction completion was determined by Kaiser ninhydrin test.<sup>23</sup> The resin was filtered, washed successively with DMF, H<sub>2</sub>O, MeOH, and dichloromethane (DCM) (3 times each), and dried in vacuo. The dried resin was then treated with 50% TFA–DCM (1 mL) for 40 min at room temperature, and the elute was concentrated under reduced pressure. The residue was dissolved in MeOH (1 mL), again concentrated, and dried in vacuo to obtain crude sample of **4**. A total of 28 out of 33 samples showed higher than 90% purity by LC-MS and HPLC spec, and even the lowest purity was found to be 71%. The products were estimated as a TFA salt (coefficient = 1) and were dissolved in DMSO for the binding assay. Because of high-throughput synthesis, it was difficult to determine the precise yields of the reaction, but generally 0.020 mmol of the starting materials (resin bound amines) gave greater than 0.015 mmol (75% yield) of the target molecule (**4**).

**Methyl (2R)-(Benzoyloxycarbonyl)pyrrolidine-2-carboxylate (**6**).** To a solution of D-benzyloxycarbonylproline **5** (7.5 g, 30 mmol) and DMAP (82 mg, 0.67 mmol) in CHCl<sub>3</sub> (20 mL) and MeOH (10 mL) was added WSC–HCl (6.9 g, 36 mmol), and the mixture was stirred at room temperature for 1 h. The reaction was quenched by adding aqueous NaHCO<sub>3</sub> solution, and the mixture was extracted with CHCl<sub>3</sub>. The organic phase was washed with H<sub>2</sub>O, dried over Na<sub>2</sub>SO<sub>4</sub>, and evaporated. The residue was purified by silica gel column chromatography (Hex–EtOAc, 6:1–4:1 elution) to give **6** (6.20 g, 23.5 mmol, 78%) as a colorless oil.

**Methyl (2R)-Pyrrolidine-2-carboxylate (**7**).** A suspension of **6** (6.20 g, 23.5 mmol) and Pd(OH)<sub>2</sub> (Degussa type, 320 mg) in MeOH (10 mL) was stirred vigorously at room temperature for 4 h under H<sub>2</sub> atmosphere. After adding Pd(OH)<sub>2</sub> (200 mg), the

suspension was stirred under the same condition for 15 h. The reaction mixture was filtered by Whatmann GF/F and the filtrate was evaporated to give the crude product of **7** (4.48 g) as a colorless oil.

**Methyl (2R)-1-[(2S,4R)-4-tert-Butoxy-1-(benzyloxycarbonyl)pyrrolidin-2-yl]carbonylpyrrolidine-2-carboxylate (8)**. To a solution of **7** (4.48 g) and *N*- $\alpha$ -benzyloxycarbonyl-*O*-*tert*-butyl-L-4-*trans*-hydroxyproline (7.55 g, 23.5 mmol) in CHCl<sub>3</sub> (30 mL) were added WSC-HCl (5.39 g, 28.2 mmol) and HOBt (4.31 g, 28.2 mmol), and the mixture was stirred for 22 h at room temperature. The reaction was quenched by adding aqueous NaHCO<sub>3</sub>, and the mixture was extracted with CHCl<sub>3</sub>. The organic phase was washed with saturated aqueous NH<sub>4</sub>Cl, dried over Na<sub>2</sub>SO<sub>4</sub>, and evaporated. The residue was purified by silica gel column chromatography (CHCl<sub>3</sub> elution) to give **8** (5.10 g, 11.8 mmol, 50% from **6**) as a colorless oil.

**Methyl (2R)-1-[(2S,4R)-4-tert-Butoxy-1-pyrrolidin-2-yl]carbonylpyrrolidine-2-carboxylate (9)**. The suspension of **8** (5.10 g, 11.8 mmol) and Pd(OH)<sub>2</sub> (Degussa type, 400 mg) in MeOH (12 mL) was stirred vigorously at room temperature for 3 h under H<sub>2</sub> atmosphere. After adding Pd(OH)<sub>2</sub> (200 mg), the suspension was stirred under the same condition for 3 h. The reaction mixture was filtered by Whatmann GF/F, and the filtrate was evaporated to give the crude product of **9** (3.54 g) as a white solid.

**Methyl (2R)-1-[(2S,4R)-4-tert-Butoxy-1-[3,3,3-tris(4-fluorophenyl)propanoyl]pyrrolidine-2-yl]carbonylpyrrolidine-2-carboxylate (11)**. To a solution of **9** (2.84 g, 9.52 mmol), and DIEA (1.99 mL, 11.4 mmol) in CHCl<sub>3</sub> (40 mL) were added WSC-HCl (2.18 g, 11.4 mmol) and HOBt (1.74 g, 11.4 mmol), and the mixture was stirred at room temperature for 13 h. The reaction was quenched by adding aqueous NaHCO<sub>3</sub>, and the mixture was extracted with CHCl<sub>3</sub>. The organic phase was washed with saturated aqueous NH<sub>4</sub>Cl, dried over Na<sub>2</sub>SO<sub>4</sub>, and evaporated. The residue was purified by silica gel column chromatography (CHCl<sub>3</sub> elution) to give **11** (5.17 g, 8.12 mmol, 86% from **8**) as a white foam.

**(2R)-1-[(2S,4R)-4-tert-Butoxy-1-[3,3,3-tris(4-fluorophenyl)propanoyl]pyrrolidine-2-yl]carbonylpyrrolidine-2-carboxylic Acid (12)**. To a solution of **11** (3.14 g, 4.93 mmol) in MeOH (10 mL) was added aqueous NaOH solution (4 mol/L, 3 mL), and the mixture was stirred at room temperature for 40 min. The reaction mixture was acidified to pH = 1 with aqueous HCl and extracted with CHCl<sub>3</sub>. The organic phase was dried over Na<sub>2</sub>SO<sub>4</sub> and evaporated to give the crude product **12** (3.24 g) as a white foam.

**(2R)-1-[(2S,4R)-4-tert-Butoxy-1-[3,3,3-tris(4-fluorophenyl)propanoyl]pyrrolidine-2-yl]carbonyl-N-[4-(tert-butoxycarbonyl)piperidinylmethyl]pyrrolidine-2-carboxamide (13)**. To a solution of **12** (3.24 g) and 4-aminomethyl-*tert*-butoxycarbonylpiperidine<sup>14</sup> (1.16 g, 5.42 mmol) in CHCl<sub>3</sub> (20 mL) were added WSC-HCl (1.13 g, 5.92 mmol) and HOBt (0.91 g, 5.9 mmol), and the mixture was stirred at room temperature for 22 h. The reaction was quenched by adding aqueous NaHCO<sub>3</sub>, and the mixture was extracted with CHCl<sub>3</sub>. The organic phase was washed with saturated aqueous NH<sub>4</sub>Cl, dried over Na<sub>2</sub>SO<sub>4</sub>, and evaporated. The residue was purified by silica gel column chromatography (CHCl<sub>3</sub>-MeOH, 500:3-500:6 elution) to give **13** (3.43 g, 4.19 mmol, 85% from **12**) as a white foam.

**(2R)-1-[(2S,4R)-4-Hydroxy-1-[3,3,3-tris(4-fluorophenyl)propanoyl]pyrrolidine-2-yl]carbonyl-N-(4-piperidinylmethyl)pyrrolidine-2-carboxamide (14a)**. TFA (4 mL) was added to **13** (3.40 g, 4.15 mmol) at 0 °C, and the mixture was stirred at room temperature for 1 h. To the reaction mixture was added TFA (2 mL), and the mixture was stirred at room temperature for an additional 2 h. The reaction mixture was basified to pH = 10 with aqueous NaOH solution and extracted with CHCl<sub>3</sub>. The organic phase was washed with H<sub>2</sub>O ( $\times$ 2), and dried over Na<sub>2</sub>SO<sub>4</sub>. The solvent was evaporated to give the crude product **14a** (2.67 g, including H<sub>2</sub>O) as a white foam. The analytical sample was prepared by drying the crude product in vacuo at 45 °C: mp 144.5-146.0

°C; HPLC *t*<sub>R</sub> = 15.3 min (system A), 21.8 min (system B); <sup>1</sup>H NMR (CDCl<sub>3</sub>)  $\delta$  0.80-2.08 (m, 12H), 2.28-2.45 (m, 2H), 2.46-2.57 (m, 2H), 2.98-3.12 (m, 4H), 3.32-3.40 (m, 1H), 3.44 (d, *J* = 15.1 Hz, 1H), 3.59 (dd, *J* = 4.1, 10.8 Hz, 1H), 3.69 (d, *J* = 15.1 Hz, 1H), 3.77-3.87 (m, 1H), 4.40-4.51 (m, 2H), 4.53-4.61 (m, 1H), 6.96 (dd, *J*<sub>HF</sub> = 8.8 Hz, *J*<sub>HH</sub> = 8.8 Hz, 6H), 7.08-7.20 (m, 1H), 7.15 (dd, *J*<sub>HF</sub> = 5.2 Hz, *J*<sub>HH</sub> = 8.8 Hz, 6H); HRMS Calcd for C<sub>37</sub>H<sub>42</sub>N<sub>4</sub>O<sub>4</sub>F<sub>3</sub> (M + H)<sup>+</sup>: 663.3158, Found: 663.3154. Anal. (C<sub>37</sub>H<sub>41</sub>N<sub>4</sub>O<sub>4</sub>F<sub>3</sub>·2.5H<sub>2</sub>O) C, H, N.

**Tris(4-fluorophenyl)propionitrile (17)**. A ZnCl<sub>2</sub> solution (1 M Et<sub>2</sub>O solution, 16.9 mL, 16.9 mmol) was coevaporated three times with toluene. Cyanoacetic acid (5.41 g, 63.6 mmol) was also coevaporated three times with toluene in another flask. A mixture of tris(4-fluorophenyl)methanol (**16**, 10.0 g, 31.8 mmol), ZnCl<sub>2</sub>, and cyanoacetic acid in acetic acid (10.9 mL, 191 mmol) was refluxed at 130 °C for 6.5 h. After the suspension was cooled to room temperature, H<sub>2</sub>O (ca. 30 mL) was added, and the mixture was extracted with CHCl<sub>3</sub>. The organic phase was dried over Na<sub>2</sub>SO<sub>4</sub> and evaporated. The residue was purified by silica gel column chromatography (Hex-EtOAc, 8:0-8:1 elution) and crystallized from Hex-EtOAc to give **17** (5.56 g, 16.5 mmol, 52%) as a white solid.

**Tris(4-fluorophenyl)propionic Acid (10)**. To a suspension of **17** (5.56 g, 16.5 mmol) in acetic acid (50 mL) were added concentrated hydrochloric acid (20 mL) and concentrated sulfuric acid (10 mL), and the mixture was refluxed at 130 °C for 44 h. The reaction mixture was cooled slowly to 0 °C, and the resultant precipitate was filtered off and washed with H<sub>2</sub>O. The precipitate was dissolved in CHCl<sub>3</sub>, and the organic layer was washed with H<sub>2</sub>O ( $\times$ 2), dried over Na<sub>2</sub>SO<sub>4</sub>, and evaporated to give **10** (5.26 g, 14.8 mmol, 90%) as a pale yellow solid.

Compounds **2a**, **51a-51c**, **52a-52c**, **14b**, and **14c** were prepared according to the synthesis of **14a**, using the appropriate triphenylpropionic acids (commercially available triphenylpropionic acid or commercially available tris(4-chlorophenyl)propionic acid), and appropriate diamine core parts ((3S)-3-aminomethyl-1-*tert*-butoxycarbonylpiperidine,<sup>24</sup> 4-aminomethyl-*tert*-butoxycarbonylpiperidine,<sup>14</sup> or 4-aminoethyl-*tert*-butoxycarbonylpiperidine.<sup>25</sup>)

**(2R)-1-[(2S,4R)-4-Hydroxy-1-(3,3,3-triphenylpropanoyl)pyrrolidine-2-yl]carbonyl-N-((3S)-3-piperidinylmethyl)pyrrolidine-2-carboxamide (2a)**. mp 92-95 °C; HPLC *t*<sub>R</sub> = 14.6 min (system A), 20.5 min (system B); <sup>1</sup>H NMR (CDCl<sub>3</sub>)  $\delta$  0.93-1.08 (m, 1H), 1.32-1.50 (m, 1H), 1.51-2.05 (m, 10H), 2.09 (t, *J* = 11.1 Hz, 1H), 2.23-2.32 (m, 1H), 2.51 (dt, *J* = 2.3, 9.6 Hz, 1H), 2.57-2.68 (m, 1H), 2.74 (d, *J* = 10.9 Hz, 1H), 2.85-3.02 (m, 3H), 3.30-3.33 (m, 1H), 3.42 (d, *J* = 14.6 Hz, 1H), 3.58 (dd, *J* = 4.1, 11.0 Hz, 1H), 3.80-3.87 (m, 1H), 3.90 (d, *J* = 14.6 Hz, 1H), 4.30-4.38 (m, 2H), 4.56 (d, *J* = 6.9 Hz, 1H), 7.17-7.32 (m, 16H); HRMS Calcd for C<sub>37</sub>H<sub>45</sub>N<sub>4</sub>O<sub>4</sub> (M + H)<sup>+</sup>: 609.3441, Found: 609.3420.

**(2R)-1-[(2S,4R)-4-Hydroxy-1-(3,3,3-triphenylpropanoyl)pyrrolidine-2-yl]carbonyl-N-(4-piperidinylmethyl)pyrrolidine-2-carboxamide (51a)**. mp 95.0-98.5 °C; HPLC *t*<sub>R</sub> = 14.1 min (system A), 19.9 min (system B); <sup>1</sup>H NMR (CDCl<sub>3</sub>)  $\delta$  1.18-1.72 (m, 6H), 1.75-2.09 (m, 5H), 2.19-2.30 (m, 1H), 2.57-2.76 (m, 3H), 2.86 (d, *J* = 10.6 Hz, 1H), 3.00-3.12 (m, 1H), 3.18-3.40 (m, 3H), 3.52 (d, *J* = 14.8 Hz, 1H), 3.57 (dd, *J* = 4.0, 11.0 Hz, 1H), 3.78 (d, *J* = 14.8 Hz, 1H), 3.79-3.86 (m, 2H), 4.30-4.40 (m, 2H), 4.50-4.59 (m, 1H), 7.13-7.32 (m, 15H), 7.33-7.41 (m, 1H); HRMS Calcd for C<sub>37</sub>H<sub>45</sub>N<sub>4</sub>O<sub>4</sub> (M + H)<sup>+</sup>: 609.3441, Found: 609.3420.

**(2R)-1-[(2S,4R)-4-Hydroxy-1-(3,3,3-triphenylpropanoyl)pyrrolidine-2-yl]carbonyl-N-(4-piperidinylethyl)pyrrolidine-2-carboxamide (51b)**. HPLC *t*<sub>R</sub> = 14.1 min (system A), 19.9 min (system B); <sup>1</sup>H NMR (CDCl<sub>3</sub>)  $\delta$  1.02-2.40 (m, 15H), 2.52-2.64 (m, 2H), 2.65-2.78 (m, 1H), 2.85 (d, *J* = 10.8 Hz, 1H), 3.02-3.11 (m, 2H), 3.12-3.24 (m, 1H), 3.29-3.40 (m, 1H), 3.45 (d, *J* = 14.6 Hz, 1H), 3.58 (dd, *J* = 4.0, 10.9 Hz, 1H), 3.78-3.82 (m, 1H), 3.83 (d, *J* = 14.6 Hz, 1H), 4.32-4.40 (m, 2H), 4.52-4.59 (m, 1H), 7.12-7.31 (m, 16H); HRMS Calcd for C<sub>38</sub>H<sub>47</sub>N<sub>4</sub>O<sub>4</sub> (M + H)<sup>+</sup>: 623.3597, Found: 623.3586.



(2R)-1-[(2S,4R)-4-Hydroxy-1-(3,3,3-triphenylpropanoyl)pyrrolidine-2-yl]carbonyl-N-((3R)-3-piperidinylmethyl)pyrrolidine-2-carboxamide (51c). mp 86–89 °C; HPLC *t<sub>R</sub>* = 14.3 min (system A), 20.1 min (system B); <sup>1</sup>H NMR (CDCl<sub>3</sub>) δ 0.88–1.05 (m, 1H), 1.17–1.43 (m, 2H), 1.45–2.08 (m, 9H), 2.21 (t, *J* = 11.0 Hz, 1H), 2.27–2.36 (m, 1H), 2.46–2.58 (m, 2H), 2.78–2.99 (m, 3H), 3.00–3.12 (m, 1H), 3.30–3.40 (m, 1H), 3.44 (d, *J* = 14.7 Hz, 1H), 3.62 (dd, *J* = 4.0, 10.9 Hz, 1H), 3.78–3.85 (m, 1H), 3.86 (d, *J* = 14.7 Hz, 1H), 4.30–4.40 (m, 2H), 4.55–4.62 (m, 1H), 7.15–7.38 (m, 16H); HRMS Calcd for C<sub>37</sub>H<sub>45</sub>N<sub>4</sub>O<sub>4</sub> (M + H)<sup>+</sup>: 609.3441, Found: 609.3416.

(2R)-1-((2S,4R)-4-Hydroxy-1-[3,3,3-tris(4-chlorophenyl)propanoyl]pyrrolidine-2-yl)carbonyl-N-(4-piperidinylmethyl)pyrrolidine-2-carboxamide (52a). mp 138–140 °C; HPLC *t<sub>R</sub>* = 17.9 min (system A), 25.3 min (system B); <sup>1</sup>H NMR (CDCl<sub>3</sub>) δ 0.83–2.08 (m, 12H), 2.29–2.45 (m, 2H), 2.46–2.58 (m, 2H), 2.98–3.16 (m, 4H), 3.30–3.38 (m, 1H), 3.39 (d, *J* = 15.0 Hz, 1H), 3.63 (dd, *J* = 4.1, 10.8 Hz, 1H), 3.71 (d, *J* = 15.0 Hz, 1H), 3.76–3.86 (m, 1H), 4.38–4.51 (m, 2H), 4.58 (d, *J* = 5.9 Hz, 1H), 7.05–7.20 (m, 1H), 7.12 (d, *J* = 8.8 Hz, 6H), 7.24 (d, *J* = 8.8 Hz, 6H); HRMS Calcd for C<sub>37</sub>H<sub>42</sub>N<sub>4</sub>O<sub>4</sub>Cl<sub>3</sub> (M + H)<sup>+</sup>: 711.2272, Found: 711.2261.

(2R)-1-((2S,4R)-4-Hydroxy-1-[3,3,3-tris(4-chlorophenyl)propanoyl]pyrrolidine-2-yl)carbonyl-N-(4-piperidylethyl)pyrrolidine-2-carboxamide (52b). mp 124–127 °C; HPLC *t<sub>R</sub>* = 17.9 min (system A), 25.4 min (system B); <sup>1</sup>H NMR (CDCl<sub>3</sub>) δ 0.95–1.88 (m, 10H), 1.90–2.00 (m, 2H), 2.01–2.12 (m, 2H), 2.28–2.38 (m, 1H), 2.46–2.60 (m, 3H), 2.98–3.11 (m, 3H), 3.20–3.38 (m, 2H), 3.40 (d, *J* = 15.4 Hz, 1H), 3.63 (dd, *J* = 4.1, 11.0 Hz, 1H), 3.71 (d, *J* = 15.4 Hz, 1H), 3.73–3.82 (m, 1H), 4.39–4.52 (m, 2H), 4.53–4.60 (m, 1H), 6.98–7.05 (m, 1H), 7.10 (d, *J* = 8.8 Hz, 6H), 7.23 (d, *J* = 8.8 Hz, 6H); HRMS Calcd for C<sub>38</sub>H<sub>44</sub>N<sub>4</sub>O<sub>4</sub>Cl<sub>3</sub> (M + H)<sup>+</sup>: 725.2428, Found: 725.2430.

(2R)-1-((2S,4R)-4-Hydroxy-1-[3,3,3-tris(4-chlorophenyl)propanoyl]pyrrolidine-2-yl)carbonyl-N-((3R)-3-piperidinylmethyl)pyrrolidine-2-carboxamide (52c). mp 132–135 °C; HPLC *t<sub>R</sub>* = 18.6 min (system A), 25.8 min (system B); <sup>1</sup>H NMR (CDCl<sub>3</sub>) δ 0.83–1.82 (m, 8H), 1.88–2.10 (m, 4H), 2.13–2.22 (m, 1H), 2.28–2.40 (m, 2H), 2.48–2.59 (m, 1H), 2.80–2.88 (m, 1H), 2.90–3.07 (m, 2H), 3.08–3.20 (m, 1H), 3.29–3.39 (m, 1H), 3.39 (d, *J* = 15.3 Hz, 1H), 3.60–3.66 (m, 1H), 3.73 (d, *J* = 15.3 Hz, 1H), 3.77–3.86 (m, 1H), 4.39–4.52 (m, 2H), 4.57 (d, *J* = 5.6 Hz, 1H), 7.02–7.20 (m, 1H), 7.12 (d, *J* = 8.9 Hz, 6H), 7.24 (d, *J* = 8.9 Hz, 6H); HRMS Calcd for C<sub>37</sub>H<sub>42</sub>N<sub>4</sub>O<sub>4</sub>Cl<sub>3</sub> (M + H)<sup>+</sup>: 711.2272, Found: 711.2269.

(2R)-1-((2S,4R)-4-Hydroxy-1-[3,3,3-tris(4-fluorophenyl)propanoyl]pyrrolidine-2-yl)carbonyl-N-(4-piperidylethyl)pyrrolidine-2-carboxamide (14b). HPLC *t<sub>R</sub>* = 15.3 min (system A), 21.7 min (system B); <sup>1</sup>H NMR (CDCl<sub>3</sub>) δ 0.85–1.86 (m, 10H), 1.88–2.00 (m, 2H), 2.00–2.10 (m, 2H), 2.27–2.36 (m, 1H), 2.47–2.60 (m, 3H), 2.98–3.06 (m, 2H), 3.07–3.14 (m, 1H), 3.15–3.28 (m, 1H), 3.30–3.41 (m, 1H), 3.45 (d, *J* = 15.5 Hz, 1H), 3.60 (dd, *J* = 4.2, 10.6 Hz, 1H), 3.70 (d, *J* = 15.5 Hz, 1H), 3.75–3.85 (m, 1H), 4.41–4.52 (m, 2H), 4.53–4.60 (m, 1H), 6.94 (dd, *J<sub>HF</sub>* = 8.5 Hz, *J<sub>HH</sub>* = 8.5 Hz, 6H), 7.00–7.10 (m, 1H), 7.13 (dd, *J<sub>HF</sub>* = 5.3 Hz, *J<sub>HH</sub>* = 8.5 Hz, 6H); HRMS Calcd for C<sub>38</sub>H<sub>44</sub>N<sub>4</sub>O<sub>4</sub>F<sub>3</sub> (M + H)<sup>+</sup>: 677.3315, Found: 677.3314.

(2R)-1-((2S,4R)-4-Hydroxy-1-[3,3,3-tris(4-fluorophenyl)propanoyl]pyrrolidine-2-yl)carbonyl-N-((3R)-3-piperidinylmethyl)pyrrolidine-2-carboxamide (14c). mp 137.0–139.5 °C; HPLC *t<sub>R</sub>* = 15.8 min (system A), 22.1 min (system B); <sup>1</sup>H NMR (CDCl<sub>3</sub>) δ 0.85–2.10 (m, 12H), 2.12–2.23 (m, 1H), 2.25–2.40 (m, 2H), 2.47–2.58 (m, 1H), 2.80–2.90 (m, 1H), 2.91–3.00 (m, 1H), 3.04–3.18 (m, 2H), 3.30–3.42 (m, 1H), 3.45 (d, *J* = 15.4 Hz, 1H), 3.62 (dd, *J* = 4.3, 10.9 Hz, 1H), 3.72 (d, *J* = 15.4 Hz, 1H), 3.77–3.85 (m, 1H), 4.40–4.50 (m, 2H), 4.52–4.60 (m, 1H), 6.96 (dd, *J<sub>HF</sub>* = 8.9 Hz, *J<sub>HH</sub>* = 8.9 Hz, 6H), 7.09–7.20 (m, 1H), 7.15 (dd, *J<sub>HF</sub>* = 5.3 Hz, *J<sub>HH</sub>* = 8.9 Hz, 6H); HRMS Calcd for C<sub>37</sub>H<sub>42</sub>N<sub>4</sub>O<sub>4</sub>F<sub>3</sub> (M + H)<sup>+</sup>: 663.3158, Found: 663.3168. Anal. (C<sub>37</sub>H<sub>41</sub>N<sub>4</sub>O<sub>4</sub>F<sub>3</sub>·3H<sub>2</sub>O) C, H, N.

N-Alkylated tertiary amine derivatives, 15a–15g, were prepared according to either method A or method B.

**Method A (Reductive Amination):** (2R)-1-((2S,4R)-4-Hydroxy-1-[3,3,3-tris(4-fluorophenyl)propanoyl]pyrrolidine-2-yl)carbonyl-N-(1-methyl-4-piperidinylmethyl)pyrrolidine-2-carboxamide (15a). To a solution of 14a (202 mg, 0.305 mmol) and formaldehyde (37% aqueous solution 200 μL) in MeOH (2 mL) was added NaBH<sub>3</sub>CN–ZnCl<sub>2</sub> (0.3 mol/L, 1.22 mL),<sup>15</sup> and the mixture was stirred at room temperature for 20 min. The reaction was quenched by adding saturated aqueous NaHCO<sub>3</sub> solution, and extracted with EtOAc. The organic phase was washed with brine, dried (NaSO<sub>4</sub>), and evaporated. The residue was purified by preparative TLC (CHCl<sub>3</sub>–MeOH–28% aqueous NH<sub>3</sub> solution, 8:1:0.1 elution) to give 15a (184 mg, 0.272 mmol, 89%) as a white foam: mp 140–142 °C; HPLC *t<sub>R</sub>* = 15.5 min (system A), 21.6 min (system B); <sup>1</sup>H NMR (CDCl<sub>3</sub>) δ 1.12–2.20 (m, 13H), 2.31 (s, 3H), 2.32–2.39 (m, 1H), 2.48–2.58 (m, 1H), 2.83–2.94 (m, 2H), 2.99–3.10 (m, 2H), 3.35–3.42 (m, 1H), 3.45 (d, *J* = 15.0 Hz, 1H), 3.62 (dd, *J* = 4.1, 11.0 Hz, 1H), 3.73 (d, *J* = 15.0 Hz, 1H), 3.78–3.88 (m, 1H), 4.40–4.53 (m, 2H), 4.59 (d, *J* = 5.9 Hz, 1H), 6.92–7.03 (m, 6H), 7.08–7.25 (m, 7H); HRMS Calcd for C<sub>38</sub>H<sub>44</sub>N<sub>4</sub>O<sub>4</sub>F<sub>3</sub> (M + H)<sup>+</sup>: 677.3315, Found: 677.3312. Anal. (C<sub>38</sub>H<sub>43</sub>N<sub>4</sub>O<sub>4</sub>F<sub>3</sub>·H<sub>2</sub>O) C, H, N.

**Method B (Alkylation):** (2R)-N-(1-Cyclopentyl-4-piperidinylmethyl)-1-((2S,4R)-4-hydroxy-1-[3,3,3-tris(4-fluorophenyl)propanoyl]pyrrolidine-2-yl)carbonylpyrrolidine-2-carboxamide (15g). To a solution of 14a (19.7 mg, 0.0297 mmol) in CH<sub>3</sub>CN (1.5 mL) were added bromocyclopentane (32 μL, 0.297 mmol) and K<sub>2</sub>CO<sub>3</sub> (12 mg, 0.089 mmol), and the mixture was stirred at 80 °C for 15 h. The reaction was quenched by adding H<sub>2</sub>O, and extracted with CHCl<sub>3</sub>. The organic phase was washed with diluted aqueous NaOH solution, dried (Na<sub>2</sub>SO<sub>4</sub>), and evaporated. The residue was purified by preparative TLC (CHCl<sub>3</sub>–MeOH–28% aqueous NH<sub>3</sub> solution, 10:1:0.1 elution) to give 15g (20 mg, 0.027 mmol, 90%) as a white foam; HPLC *t<sub>R</sub>* = 16.9 min (system A), 22.5 min (system B); <sup>1</sup>H NMR (CDCl<sub>3</sub>) δ 1.08–2.20 (m, 21H), 2.29–2.65 (m, 3H), 3.02–3.18 (m, 4H), 3.30–3.92 (m, 3H), 3.42 (d, *J* = 15.2 Hz, 1H), 3.71 (d, *J* = 15.2 Hz, 1H), 4.39–4.67 (m, 3H), 6.90–7.27 (m, 13H); HRMS Calcd for C<sub>42</sub>H<sub>50</sub>N<sub>4</sub>O<sub>4</sub>F<sub>3</sub> (M + H)<sup>+</sup>: 731.3784, Found: 731.3799.

(2R)-N-(1-Ethyl-4-piperidinylmethyl)-1-((2S,4R)-4-hydroxy-1-[3,3,3-tris(4-fluorophenyl)propanoyl]pyrrolidine-2-yl)carbonylpyrrolidine-2-carboxamide (15b). Yield 52% (Method B); mp 97–99 °C; HPLC *t<sub>R</sub>* = 15.8 min (system A), 21.6 min (system B); <sup>1</sup>H NMR (CDCl<sub>3</sub>) δ 1.03–2.15 (m, 16H), 2.29–2.48 (m, 3H), 2.50–2.60 (m, 1H), 2.86–2.96 (m, 2H), 2.97–3.10 (m, 2H), 3.30–3.40 (m, 1H), 3.42 (d, *J* = 15.1 Hz, 1H), 3.63 (dd, *J* = 3.9, 11.0 Hz, 1H), 3.72 (d, *J* = 15.1 Hz, 1H), 3.78–3.88 (m, 1H), 4.40–4.52 (m, 2H), 4.53–4.61 (m, 1H), 6.96 (dd, *J<sub>HF</sub>* = 8.8 Hz, *J<sub>HH</sub>* = 8.8 Hz, 6H), 7.07–7.20 (m, 1H), 7.16 (dd, *J<sub>HF</sub>* = 5.3 Hz, *J<sub>HH</sub>* = 8.8 Hz, 6H); HRMS Calcd for C<sub>39</sub>H<sub>46</sub>N<sub>4</sub>O<sub>4</sub>F<sub>3</sub> (M + H)<sup>+</sup>: 691.3471, Found: 691.3475.

(2R)-N-(1-Cyclopropylmethyl-4-piperidinylmethyl)-1-((2S,4R)-4-hydroxy-1-[3,3,3-tris(4-fluorophenyl)propanoyl]pyrrolidine-2-yl)carbonylpyrrolidine-2-carboxamide (15c). Yield 91% (Method A); mp 103.5–106 °C; HPLC *t<sub>R</sub>* = 16.6 min (system A), 22.3 min (system B); <sup>1</sup>H NMR (CDCl<sub>3</sub>) δ 0.06–0.20 (m, 2H), 0.48–0.60 (m, 2H), 0.80–0.95 (m, 2H), 1.10–2.13 (m, 11H), 2.22–2.40 (m, 3H), 2.48–2.58 (m, 1H), 2.98–3.20 (m, 4H), 3.30–3.52 (m, 1H), 3.43 (d, *J* = 15.3 Hz, 1H), 3.58–3.90 (m, 3H), 3.72 (d, *J* = 15.3 Hz, 1H), 4.40–4.64 (m, 3H), 6.96 (dd, *J<sub>HF</sub>* = 8.7 Hz, *J<sub>HH</sub>* = 8.7 Hz, 6H), 7.07–7.26 (m, 1H), 7.15 (dd, *J<sub>HF</sub>* = 5.2 Hz, *J<sub>HH</sub>* = 8.7 Hz, 6H); HRMS Calcd for C<sub>41</sub>H<sub>48</sub>N<sub>4</sub>O<sub>4</sub>F<sub>3</sub> (M + H)<sup>+</sup>: 717.3628, Found: 717.3606.

(2R)-N-(1-Cyclobutylmethyl-4-piperidinylmethyl)-1-((2S,4R)-4-hydroxy-1-[3,3,3-tris(4-fluorophenyl)propanoyl]pyrrolidine-2-yl)carbonylpyrrolidine-2-carboxamide (15d). Yield 84% (Method B); HPLC *t<sub>R</sub>* = 17.2 min (system A), 22.9 min (system B); <sup>1</sup>H NMR (CDCl<sub>3</sub>) δ 0.82–2.10 (m, 20H), 2.28–2.44 (m, 2H), 2.45–2.60 (m, 2H), 2.76–2.92 (m, 2H), 2.97–3.08 (m, 2H), 3.30–3.40 (m, 1H), 3.41 (d, *J* = 15.1 Hz, 1H), 3.57–3.67 (m, 1H), 3.72 (d, *J* = 15.1 Hz, 1H), 3.78–3.87 (m, 1H), 4.39–4.52 (m, 2H), 4.54–3.61 (m, 1H), 6.96 (dd, *J<sub>HF</sub>* = 8.8 Hz, *J<sub>HH</sub>* = 8.8 Hz, 6H), 7.06–

7.20 (m, 1H), 7.15 (dd,  $J_{\text{HF}} = 5.3$  Hz,  $J_{\text{HH}} = 8.8$  Hz, 6H); HRMS Calcd for  $\text{C}_{42}\text{H}_{50}\text{N}_4\text{O}_4\text{F}_3$  ( $\text{M} + \text{H}$ ) $^+$ : 731.3784, Found: 731.3797.

(2R)-N-(1-Cyclopentylmethyl-4-piperidinylmethyl)-1-(2S,4R)-4-hydroxy-1-[3,3,3-tris(4-fluorophenyl)propanoyl]pyrrolidine-2-yl)carbonylpyrrolidine-2-carboxamide (15e). Yield 68% (Method B); HPLC  $t_{\text{R}} = 17.8$  min (system A), 23.4 min (system B);  $^1\text{H}$  NMR ( $\text{CDCl}_3$ )  $\delta$  1.07–2.50 (m, 26H), 2.82–2.98 (m, 2H), 3.00–3.12 (m, 2H), 3.32–3.40 (m, 1H), 3.44 (d,  $J = 15.2$  Hz, 1H), 3.62 (dd,  $J = 4.3$ , 10.8 Hz, 1H), 3.72 (d,  $J = 15.2$  Hz, 1H), 3.78–3.88 (m, 1H), 4.40–4.52 (m, 2H), 4.53–4.61 (m, 1H), 6.96 (dd,  $J_{\text{HF}} = 8.8$  Hz,  $J_{\text{HH}} = 8.8$  Hz, 6H), 7.07–7.22 (m, 1H), 7.15 (dd,  $J_{\text{HF}} = 5.2$  Hz,  $J_{\text{HH}} = 8.8$  Hz, 6H); HRMS Calcd for  $\text{C}_{43}\text{H}_{52}\text{N}_4\text{O}_4\text{F}_3$  ( $\text{M} + \text{H}$ ) $^+$ : 745.3941, Found: 745.3953.

(2R)-1-(2S,4R)-4-Hydroxy-1-[3,3,3-tris(4-fluorophenyl)propanoyl]pyrrolidine-2-yl)carbonyl-N-[1-(2-propyl)-4-piperidinylmethyl]pyrrolidine-2-carboxamide (15f). Yield quant. (Method B); HPLC  $t_{\text{R}} = 16.1$  min (system A), 21.8 min (system B);  $^1\text{H}$  NMR ( $\text{CDCl}_3$ )  $\delta$  0.82–2.17 (m, 13H), 1.06 (d,  $J = 6.2$  Hz, 6H), 2.28–2.37 (m, 1H), 2.48–2.59 (m, 1H), 2.66–2.93 (m, 3H), 2.96–3.10 (m, 2H), 3.32–3.41 (m, 1H), 3.43 (d,  $J = 15.0$  Hz, 1H), 3.63 (dd,  $J = 4.3$ , 10.8 Hz, 1H), 3.73 (d,  $J = 15.0$  Hz, 1H), 3.78–3.88 (m, 1H), 4.38–4.51 (m, 2H), 4.57 (d,  $J = 6.7$  Hz, 1H), 6.96 (dd,  $J_{\text{HF}} = 8.8$  Hz,  $J_{\text{HH}} = 8.8$  Hz, 6H), 7.08–7.20 (m, 1H), 7.16 (dd,  $J_{\text{HF}} = 5.4$  Hz,  $J_{\text{HH}} = 8.8$  Hz, 6H); HRMS Calcd for  $\text{C}_{40}\text{H}_{48}\text{N}_4\text{O}_4\text{F}_3$  ( $\text{M} + \text{H}$ ) $^+$ : 705.3628, Found: 705.3633.

**Alignment of Muscarinic Receptor Subtypes.** Sequence alignment of the five human muscarinic receptor subtypes with bovine rhodopsin was accomplished as shown below. Aligned muscarinic subfamilies were downloaded from GPCR database (<http://tinygrape.uit.no/>).<sup>26</sup> The alignment of rhodopsin and all muscarinic receptor subtypes was generated manually by aligning key class A sequence motifs (shown in bold in Figure 3). The lengths of the TM helices were defined as reported by Bondensgaard et al.,<sup>27</sup> and the sequence identity between  $\text{M}_3$  and rhodopsin sequences in the transmembrane helical regions is 20.9%.

**Receptor Modeling and Docking.** All molecular modeling studies were carried out on a Silicon Graphics Octane 2 workstation. The homology model of the 7 TM domain for the human  $\text{M}_3$  receptor was constructed using the homology module in Insight2000.<sup>28</sup> The bovine rhodopsin crystal structure (PDB entry 1F88)<sup>29</sup> was used as template structure for homology modeling. Loop regions as well as the C- and N-terminus were not included in the models as these regions are impossible to model accurately. The side chains were minimized to avoid steric clashes using the CHARMM force field as implemented in QUANTA.<sup>30</sup>

Since the receptor structure is only a homology model, docking was conducted by hand followed by minimization with the CHARMM program, using the CHARMM force field. The following criteria were employed to achieve meaningful docking modes: (1) The ligands would form ionic interaction between the cationic N and Asp 148 in TM3. (2) No steric clashes would happen between any two atoms. (3) The ligands would have most favorable conformations to make interactions with the key residues Asn138 in TM3, Lys523, and Asn527 in TM7. Side chain orientations were adjusted to avoid steric clashes between receptor and ligand atoms by minimization.

**Binding Assay.** According to the reported method,<sup>19</sup> the binding affinities were determined by inhibition of specific binding of [ $^3\text{H}$ ]-NMS using membranes from CHO cells expressing cloned human  $\text{M}_1$ – $\text{M}_5$  receptors.

**Functional Assay.** According to the reported method,<sup>19</sup> antagonistic activities using isolated rat tissues were evaluated.

**Acknowledgment.** We are grateful to Ms. Nami Sakaizumi, Mr. Hirokazu Ohsawa, Ms. Chihiro Sato, Ms. Aya Mitsuya, Mr. Taro Yamashita, and Ms. Miyoko Miyashita for technical support and Ms. Sandy Camburn for her valuable assistance in preparation of the manuscript.

**Supporting Information Available:** A table listing the degree of purity for all target compounds (area percent and retention time),

a table listing the elemental analysis results, spectroscopic data for the synthetic intermediates **6**–**13** and **17**, and solid phase immobilization of diverse diamine reagents using 2-chlorotriethyl chloride resin (Cl-Trt(2-Cl)-resin). This material is available free of charge via the Internet at <http://pubs.acs.org>.

## References

- (a) Kubo, T.; Fukuda, K.; Mikami, A.; Maeda, A.; Takahashi, H.; Mishina, M.; Haga, T.; Haga, K.; Ichiyama, A.; Kangawa, K.; Kojima, M.; Matsuo, H.; Hirose, T.; Numa, S. Cloning, sequencing and expression of complementary DNA encoding the muscarinic acetylcholine receptor. *Nature* **1986**, *323*, 411–416. (b) Kubo, T.; Maeda, A.; Sugimoto, K.; Akiba, I.; Mikami, A.; Takahashi, H.; Haga, T.; Haga, K.; Ichiyama, A.; Kangawa, K.; Matsuo, H.; Hirose, T.; Numa, S. Primary structure of porcine cardiac muscarinic acetylcholine receptor deduced from the cDNA sequence. *FEBS Lett.* **1986**, *209*, 367–372. (c) Peralta, E. G.; Ashkenazi, A.; Winslow, J. W.; Smith, D. H.; Ramachandran, J.; Capon, D. J. Distinct primary structures, ligand-binding properties and tissue-specific expression of four human muscarinic acetylcholine receptors. *EMBO J.* **1987**, *6*, 3923–3929. (d) Bonner, T. I.; Buckley, N. J.; Young, A. C.; Brann, M. R. Identification of a family of muscarinic acetylcholine receptor genes. *Science* **1987**, *237*, 527–532. (e) Bonner, T. I.; Young, A. C.; Brann, M. R.; Buckley, N. J. Cloning and expression of the human and rat  $\text{m}_5$  muscarinic acetylcholine receptor genes. *Neuron* **1988**, *1*, 403–410.
- (2) Caulfield, M. P.; Birdsall, N. J. M. International union of pharmacology. XII. Classification of muscarinic acetylcholine receptors. *Pharmacol. Rev.* **1998**, *50*, 279–290.
- (3) Wess, J. Muscarinic acetylcholine receptor knockout mice: novel phenotypes and clinical implications. *Annu. Rev. Pharmacol. Toxicol.* **2004**, *44*, 423–450. Wess, J. Novel insights into muscarinic acetylcholine receptor function using gene targeting technology. *Trends Pharmacol. Sci.* **2003**, *24*, 414–420. Nakamura, T.; Matusi, M.; Uchida, K.; Futatsugi, A.; Kusakawa, S.; Matsumoto, N.; Nakamura, K.; Manabe, T.; Taketo, M. M.; Mikoshiba, K.  $\text{M}_3$  muscarinic acetylcholine receptor plays a critical role in parasympathetic control of salivation in mice. *J. Physiol.* **2004**, *558*, 561–575.
- (4) (a) Eglén, R. M.; Choppin, A.; Dillon, M. P.; Hegde, S. Muscarinic receptor ligands and their therapeutic potential. *Curr. Opin. Chem. Biol.* **1999**, *3*, 426–432. (b) Andersson, K.-E. Potential benefits of muscarinic  $\text{M}_3$  receptor selectivity. *Eur. Urol., Suppl.* **2002**, *1*, 23–28.
- (5) For example, the human  $\text{M}_3$  receptor is 73–83% homologous to the other subtypes,  $\text{M}_1$ ,  $\text{M}_2$ ,  $\text{M}_4$ , and  $\text{M}_5$  in the transmembrane region. See the details in modeling part of Results and Discussion and Experimental sections.
- (6) Regarding  $\text{M}_2$  antagonists and  $\text{M}_4$  antagonists, highly selective ones have been disclosed so far. See the following recent papers and the references therein: (a) Palani, A.; Dugar, S.; Clader, J. W.; Greenlee, W. J.; Ruperto, V.; Duffy, R. A.; Lachowicz, J. E. Isopropyl amide derivatives of potent and selective muscarinic  $\text{M}_2$  receptor antagonists. *Bioorg. Med. Chem. Lett.* **2004**, *14*, 1791–1794. (b) Clader, J. W.; Billard, W.; Binch, H., III; Chen, L.-Y.; Crosby, G., Jr.; Duffy, R. A.; Ford, J.; Kozłowski, J. A.; Lachowicz, J. E.; Li, S.; Liu, C.; McCombie, S. W.; Vice, S.; Zhou, G.; Greenlee, W. J. Muscarinic  $\text{M}_2$  receptor antagonists: anthranilamide derivatives with exceptional selectivity and in vivo activity. *Bioorg. Med. Chem.* **2004**, *12*, 319–326. (c) Böhme, T. M.; Keim, C.; Kreuzmann, K.; Linder, M.; Dingermann, T.; Dannhardt, G.; Mutschler, E.; Lambrecht, G. Structure–activity relationships of dimethindene derivatives as new  $\text{M}_2$ -selective muscarinic receptor antagonists. *J. Med. Chem.* **2003**, *46*, 856–867. (d) Böhme, T. M.; Augelli-Szafran, C. E.; Hallak, H.; Pugsley, T.; Serpa, K.; Schwarz, R. D. Synthesis and pharmacology of benzoxazines as highly selective antagonists at  $\text{M}_4$  muscarinic receptors. *J. Med. Chem.* **2002**, *45*, 3094–3102.
- (7) Sagara, Y.; Sagara, T.; Mase, T.; Kimura, T.; Numazawa, T.; Fujikawa, T.; Noguchi, K.; Ohtake, N. Cyclohexylmethylpiperidinyltriphenylpropioamide: a selective muscarinic  $\text{M}_3$  antagonist discriminating against the other receptor subtypes. *J. Med. Chem.* **2002**, *45*, 984–987.
- (8) Sagara, Y.; Kimura, T.; Fujikawa, T.; Noguchi, K.; Ohtake, N. Identification of novel muscarinic  $\text{M}_3$  selective antagonists with a conformationally restricted Hyp-Pro spacer. *Bioorg. Med. Chem. Lett.* **2003**, *13*, 57–60.
- (9) Cl-Trt(2-Cl)-resin (1% divinylbenzene, 100–200 mesh, 1.2 mmol/g) was purchased from Novabiochem.
- (10) See Supporting Information for detailed information on solid phase immobilization of diverse diamine reagents using 2-chlorotriethyl chloride resin (Cl-Trt(2-Cl)-resin) and its general experimental procedures.

- (11) Coste, J.; Le-Nguyen, D.; Castro, B. PyBOP: A new peptide coupling reagent devoid of toxic byproduct. *Tetrahedron Lett.* **1990**, *31*, 205–208.
- (12) See Experimental Section for detailed information.
- (13) All new compounds were characterized by <sup>1</sup>H NMR, RP-HPLC, and mass spectra.
- (14) Prugh, J. D.; Birchenough, L. A.; Egbertson, B. A simple method of protecting a secondary amine with *tert*-butyloxycarbonyl (BOC) in the presence of a primary amine. *Synth. Commun.* **1992**, *22*, 2357–2360.
- (15) Kim, S.; Oh, C. H.; Ko, J. S.; Ahn, K. H.; Kim, Y. J. Zinc-modified cyanoborohydride as a selective reducing agent. *J. Org. Chem.* **1985**, *50*, 1927–1932.
- (16) Schoor, M. Reaction of triphenylcarbinols with cyanoacetic acid. *Justus Liebigs Ann. Chem.* **1963**, *661*, 157–164.
- (17) The best hydrolysis reaction condition was found to be the following after examination of several conditions: heating of **17** in the solution consisting of conc HCl:conc H<sub>2</sub>SO<sub>4</sub>:AcOH = 2:1:5 at 130 °C for 44 h.
- (18) The solubility of **14a** in assay buffer (50 mM Tris-HCl, 10 mM MgCl<sub>2</sub>, 1 mM EDTA, pH 7.4, see ref 19 for the detailed assay condition) was tested, and **14a** was found to be soluble in the buffer at the concentration of at least 85 μM. As the final (highest) assay concentration was 10 μM, so **14a** was thought to be soluble at any concentration during the assay.
- (19) Hirose, H.; Aoki, I.; Kimura T.; Fujikawa, T.; Numazawa, T.; Sasaki, K.; Sato, A.; Hasegawa, T.; Nishikibe, M.; Mitsuya, M.; Ohtake, N.; Mase, T.; Noguchi, K. Pharmacological properties of (2*R*)-*N*-[1-(6-aminopyridin-2-ylmethyl)piperidin-4-yl]-2-[(1*R*)-3,3-difluorocyclopentyl]-2-hydroxy-2-phenylacetamide: a novel muscarinic antagonist with M<sub>2</sub>-sparing antagonistic activity. *J. Pharmacol. Exp. Ther.* **2001**, *297*, 790–797.
- (20) pK<sub>i</sub>(M<sub>3</sub>) value of **14a**: 9.5.
- (21) The results of the functional assay using isolated rat tissues suggested that **14a** could be competitive with carbachol, a representative muscarinic agonist possessing a cationic amino core. The binding of small molecule antagonists and agonists such as carbachol to muscarinic receptors appears to be mediated by an ion–ion interaction between the amine moiety of the ligands and an aspartic residue in TM3 of the receptors (Asp148 in the human M<sub>3</sub> receptors) according to the literatures (see ref 22). Therefore, it might be reasonable to assume that ligand–receptor interaction begins with the interaction of the cationic amine moiety of **14a** and the carboxylate group of Asp148 in human M<sub>3</sub> receptors.
- (22) Wess, J.; Maggio, R.; Palmer, J. R.; Vogel, Z. Role of conserved threonine and tyrosine residues in acetylcholine binding and muscarinic receptor activation. A study with m3 muscarinic receptor point mutants. *J. Biol. Chem.* **1992**, *267*, 19313–19319. Fraser, C. M.; Wang, C.-D.; Robinson, D. A.; Gocayne, J. D.; Venter, J. C. Site-directed mutagenesis of m1 muscarinic acetylcholine receptors: conserved aspartic acids play important roles in receptor function. *Mol. Pharmacol.* **1989**, *36*, 840–847. Curtis, C. A. M.; Wheatley, M.; Bansal, S.; Birdsall, N. J. M.; Eveleigh, P.; Pedder, E. K.; Poyner, D.; Hulme, E. C. Propylbenzilylcholine mustard labels an acidic residue in transmembrane helix 3 of the muscarinic receptor. *J. Biol. Chem.* **1989**, *264*, 489–495. Kurtenbach, E.; Curtis, C. A. M.; Pedder, E. K.; Aitken, A.; Harris, A. C. M.; Hulme, E. C. Muscarinic acetylcholine receptors. Peptide sequencing identifies residues involved in antagonist binding and disulfide bond formation. *J. Biol. Chem.* **1990**, *265*, 13702–13708.
- (23) Kaiser, E.; Colescald, D. C.; Bossinger, C. D.; Cook, P. Color test for detection of free terminal amino groups in the solid phase synthesis of peptides. *Anal. Biochem.* **1970**, *34*, 595–598.
- (24) Hilpert, K.; Ackermann, J.; Banner, D. W.; Gast, A.; Gubernator, K.; Hadváry, P.; Labler, L.; Müller, K.; Schmid, G.; Tschopp, T. B.; Waterbeemd, H. Design and synthesis of potent and highly selective thrombin inhibitors. *J. Med. Chem.* **1994**, *37*, 3889–3901.
- (25) Askew, B. C.; Bednar, R. A.; Bednar, B.; Claremon, D. A.; Cook, J. J.; McIntyre, C. J.; Hunt, C. A.; Gould, R. J.; Lynch, R. J.; Lynch, J. J., Jr.; Gaul, S. L.; Stranieri, M. T.; Sitko, G. R.; Holahan, M. A.; Glass, J. D.; Hamill, T.; Gorham, L. M.; Prueksaritanont, T.; Baldwin, J. J.; Hartman, G. D. Non-peptide glycoprotein IIb/IIIa inhibitors. 17. Design and synthesis of orally active, long-acting non-peptide fibrinogen receptor antagonists. *J. Med. Chem.* **1997**, *40*, 1779–1788.
- (26) Kristiansen, K.; Dahl, S. G.; Edvardsen, Ø. A database of mutants and effects of site-directed mutagenesis experiments on G protein-coupled receptors. *PROTEINS: Struct. Funct. Genet.* **1996**, *26*, 81–94.
- (27) Bondensgaard, K.; Ankersen, M.; Thogersen, H.; Hansen, B. S.; Wulff, B. S.; Bywater, R. P. Recognition of privileged structures by G-protein coupled receptors. *J. Med. Chem.* **2004**, *47*, 888–899.
- (28) *Insight2000*; Accelrys, Inc.: San Diego, CA.
- (29) Palczewski, K.; Kumasaka, T.; Hori, T.; Behnke, C. A.; Motoshima, H.; Fox, B. A.; Le Trong, I.; Teller, D. C.; Okada, T.; Stenkamp, R. E.; Yamamoto, M.; Miyano, M. Crystal structure of rhodopsin: A G protein-coupled receptor. *Science* **2000**, *289*, 739–745.
- (30) *Quanta/CHARMm*; Accelrys, Inc.: San Diego, CA.

JM051205R